ECOGRAPHY

Research article

Model-based impact analysis of climate change and land-use intensification on trophic networks

EDITOR'S CHOICE

Christian Neumann[1], **Tuanjit Sritongchuay**[1] **and Ralf Seppelt**[1,2,3]

[1]Department Computational Landscape Ecology, UFZ – Helmholtz Centre for Environmental Research, Leipzig, Germany
[2]Institute of Geoscience and Geography, Martin-Luther-University Halle-Wittenberg, Halle (Saale), Germany
[3]iDiv – German Centre for Integrative Biodiversity Research, Leipzig, Germany

Correspondence: Christian Neumann (christian.neumann@ufz.de)

Ecography
2025: e07533
doi: 10.1111/ecog.07533
Subject Editor:
Núria Galiana Ibáñez
Editor-in-Chief: Miguel Araújo
Accepted 14 October 2024

There is well-established evidence that land use is the main driver of terrestrial biodiversity loss. In contrast, the combined effects of land-use and climate changes on food webs, particularly on terrestrial trophic networks, are understudied. In this study, we investigate the combined effects of climate change (temperature, precipitation) and land-use intensification on food webs using a process-based general mechanistic ecosystem model ('MadingleyR'). We simulated the ecosystem dynamics of four regions in different climatic zones (Brazil, Namibia, Finland and France) according to trait-based functional groups of species (ectothermic and endothermic herbivores, carnivores and omnivores). The simulation results were consistent across the selected regions, with land-use intensification negatively affecting endotherms, whereas ectotherms were under increased pressure from rising temperatures. Land-use intensification led to the downsizing of endotherms, and thus, to smaller organisms in the food web. In combination with climate change, land-use intensification had the greatest effect on higher trophic levels, culminating in the extinction of endothermic carnivores in Namibia and Finland and endothermic omnivores in Namibia. Arid and tropical regions showed a slightly higher response of total biomass to climate change under a high-emissions scenario with rising temperatures, whereas areas with low net primary productivity showed the most negative response to land-use intensification. Our results suggest that 1) further land-use intensification will significantly affect larger organisms and predators, leading to a major restructuring of global food webs. 2) Arid low-productivity regions will experience significant changes in community composition due to global change. 3) Climate changes appear to have slightly greater effects in tropical and arid climates, whereas land-use intensification tends to affect less productive environments. This paper shows how general ecosystem models deepen our understanding of multitrophic interactions and how climate change or land-use drivers affect ecosystems in different biomes.

Keywords: climate change, functional groups, global change, land use, MadingleyR, multitrophic biodiversity

NORDIC SOCIETY OIKOS

www.ecography.org

Introduction

Global change is increasingly affecting terrestrial ecosystems. Climate change-induced temperature rise, land-use changes, resource exploitation, pollution and invasive species are the main drivers affecting ecosystems (IPBES 2019, Chrysafi et al. 2022). Among these, land-use change, particularly land-use intensification, is the largest driver of biodiversity loss (Newbold et al. 2015, IPBES 2019, Beckmann et al. 2019, Jaureguiberry et al. 2022). Despite a growing body of literature investigating the combined effects of land use and climate change on terrestrial food webs (Strona and Bradshaw 2022, O'Connor et al. 2024), their effects on trophic network structures are not sufficiently understood.

Land expansion reduces food web complexity owing to range contraction-driven species extinction and the loss of food web interconnections (Fricke et al. 2022). However, land-use intensification (i.e. increased use of fertilizers, pesticides, machinery and monocultures) affects various plant and animal species groups (Gerstner et al. 2014, Newbold et al. 2015, Beckmann et al. 2019). Most of these serve as preys, resulting in indirect effects on predatory species (Botella et al. 2024, O'Connor et al. 2024). Owing to the loss of top–down control, an increase in the number of mesopredators reduces food web compartmentalization (Botella et al. 2024) and impacts species interactions (Prugh et al. 2009, Bloor et al. 2021, O'Connor et al. 2024).

Climate change-induced rising temperatures directly affect the physiology of species, as metabolic rates increase with temperature (Brown et al. 2004), and species have specific thermal tolerance ranges that determine their activity and survival (Deutsch et al. 2008, Huey et al. 2012, Kingsolver et al. 2013). Although the direct impact of precipitation on food webs seems to be buffered by diverse trophic interactions and species diversity because of increased food web complexity (Trzcinski et al. 2016), droughts can also negatively affect net primary productivity (Cao et al. 2022). This, in turn, can have a direct impact on autotrophic biomass, indirectly determining the amount of energy available at other trophic levels (Haberl et al. 2007, Rosenblatt et al. 2017).

Consequently, land-use changes combined with climate change can further reduce the resources available at all trophic levels and alter bottom–up and top–down regulatory mechanisms. For example, if the biomass available to herbivores is reduced, availability of prey for carnivores decreases, which increases coextinction (Strona and Bradshaw 2022, O'Connor et al. 2024). Habitat loss due to climatic niche shifts (Deutsch et al. 2008, Kingsolver et al. 2013, Wiens and Zelinka 2024) may be further exacerbated by human land-use change (Mantyka-pringle et al. 2012, Segan et al. 2016); species staying in environmental conditions that were closer to their climatic tolerance limits are more sensitive to changes during human-altered land-use (Williams and Newbold 2021, Williams et al. 2022).

Studying the combined effects of both drivers on biodiversity requires consideration of the diversity of functional groups of species. Although various species might be considered in an aggregated way by studying functional groups, this approach provides sufficiently detailed information which goes well beyond classical biodiversity indicators, such as the living planet index (Loh et al. 2005), biodiversity intactness index (Newbold et al. 2015), or mean species abundance (Schipper et al. 2020).

To investigate how functional species groups respond to changes in land use and climate, functional groups can be defined by species traits such as thermoregulatory mode, feeding type, dispersal strategy, population dynamics or body size. Ectotherms are expected to be particularly affected by global warming because their physiological abilities (e.g. reproduction and growth) are tied to thermal ranges (Deutsch et al. 2008, Kingsolver et al. 2013, Paaijmans et al. 2013, Burraco et al. 2020); furthermore, they cannot thermoregulate internally (Hayden Bofill and Blom 2024). Conversely, endotherms can maintain body temperature (Buckley et al. 2012, Hayden Bofill and Blom 2024) and have high energy requirements; hence, they are more dependent on primary productivity (Buckley et al. 2012, Lasmar et al. 2021). With respect to the size, larger organisms are more susceptible to land-use and climate changes because their metabolic energy requirements scale with body size and temperature (Allen et al. 2002, Brown et al. 2004). This can lead to a decrease in body size within the food web (Sheridan and Bickford 2011, Ripple et al. 2016, Enquist et al. 2020). In contrast, land-use intensity (Munn et al. 2013, Santini and Isaac 2021), or environmental conditions (Antunes et al. 2023) may change the typically negative relationship that abundance declines with increasing body mass, described by the power law of abundance–body mass scaling (Blackburn and Gaston 1999, White et al. 2007, Lewis et al. 2008).

The removal of vegetation through land-use changes or droughts can reduce the biomass of autotrophic organisms, which can disproportionately impact higher trophic levels by reducing prey availability (Barnes et al. 2017, Rosenblatt et al. 2017, Newbold et al. 2020a, b). The environmental conditions of the habitats also play an important role. Rising ambient temperatures particularly affect tropical ectotherms that are located in areas with conditions close to their critical temperature maxima, rather than temperate ectotherms (Deutsch et al. 2008, Huey et al. 2012, Kingsolver et al. 2013). Less productive, arid environments may be disrupted, particularly because of land-use changes, as organisms have fewer opportunities to acquire food through dispersal (Newbold et al. 2020b).

The complex effects of land-use and climate changes on different functional groups of organisms illustrate the importance of studying them across multiple trophic groups, ecosystems, and climatic zones. Hence, we aimed to test the following hypotheses across four regions with different climate zones, namely, Brazil, Finland, France and Namibia.

1) Ectotherms are particularly affected by rising temperatures because of climate change.
2) Large organisms are particularly affected by the increasing pressure from climate change and land-use intensification.

3) Top predators experience disproportionate losses owing to indirect pressures from land-use intensification, which may lead to a mesopredator release.
4) Organisms in tropical and arid regions are more affected by increasing temperatures because of climate change than organisms in other climatic zones.

To examine the combined effects of climate change and land-use intensification on the functional groups of species at different trophic levels in detail, we used a general mechanistic ecosystem model (GEM). Although food web–land use interactions (Newbold et al. 2020b) or consequences of trophic rewilding (Hoeks et al. 2023) have been studied, to the best of our knowledge, there has been no model-based investigation to simulate combined interactions of food web, climate change and land-use interactions using a GEM (Pilowsky et al. 2022). Process-based GEMs provide insights into ecosystem food web dynamics such as trophic network interactions, food web energy flux, population, and trait-based dynamics (Harfoot et al. 2014, Hoeks et al. 2021, Pilowsky et al. 2022). GEMs allow the study of the effects of climate and land-use changes on ecosystem functions and processes (Harfoot et al. 2014, Newbold et al. 2020b) by capturing the interactions in trophic networks (e.g. predator–prey interactions) using an individual-based approach.

Material and methods

Study areas and input data

We used coupled model intercomparison project phase 6 (CMIP6) climate grid data at a 0.5-degree resolution from the CNRM-CM6-1-HR model simulations. The variables that influenced functional groups, namely, precipitation, temperature (2 m above the surface, diurnal temperature range), and net primary productivity (NPP), were obtained. The CMIP6 historical scenarios from 1850 to 2014, based on real-world observations (Voldoire 2019a) served as the baseline for further shared socioeconomic pathway simulations in ScenarioMIP (Eyring et al. 2016). To gain insight into different temperature trajectories, we used the future climate scenarios SSP1-2.6 (Voldoire 2019b) and SSP5-8.5 (Voldoire 2019c). SSP1-2.6 was used as the "most sustainable SSP" with temperature change remaining well below 2°C by 2100 (O'Neill et al. 2016). SSP5-8.5 was considered for the high-emissions, fossil-fuel-based scenario, with global surface temperature projected to rise to 5.7°C by the end of the century (IPCC 2021).

For each climate scenario, 30-year averages were calculated, i.e. the average across 1984–2014 for the historical climate data and that across 2070–2100 for the two future climate scenarios. This accounted for climatic variability and the averaging of single extreme events. Further details on the preprocessing of climate data can be found in the Supporting information.

Four regions across Brazil, Namibia, France and Finland were selected to study climate change and land-use impacts (Table 1). To gain insights into the regional effects of climate change, the extent of each region was selected based on the climate zone according to the current Köppen–Geiger climate classification scheme (Beck et al. 2018). To assess regions affected by different extents of land use, the regions further differed in their current human appropriation of net primary productivity (HANPP), with lower pressure in Namibia, intermediate pressure in Brazil and Finland, and higher pressure in France (Table 1).

General mechanistic ecosystem model – 'MadingleyR'

Mechanistic, process-based ecosystem models simulate ecosystem dynamics based on fundamental ecological principles and the ensuing processes (Cabral et al. 2017), such as the metabolic theory of ecology (Brown et al. 2004). A mechanistic model can be described as general if it aims to simulate the processes of any ecosystem (terrestrial or marine) independent of the scale (Harfoot et al. 2014).

Table 1. Extent, human appropriation of net primary productivity (HANPP), near-surface temperature, precipitation, and net primary productivity (NPP) for the different climate scenarios in each region included in the study. Climate zones were selected based on the current Köppen–Geiger climate classification scheme (Beck et al. 2018). Brazil is set in a tropical climate (Af), Namibia in an arid climate (BSh), France in a temperate climate (Cfb), and Finland in a cold climate (Dfc).

Area (climate zone)	Extent in terms of latitude and longitude (min., max.) (0.5° resolution)	Mean annual near-surface temperature (°C)	Mean annual precipitation (mm month^{-1})	Mean annual NPP productivity (g C m^{-2} day^{-1})	Mean HANPP (g C m^{-2} year^{-1})
Brazil (Af)	Lat.: 3°0′0″S, 0°0′ 0″N Lon.: 69°0′0″W, 61°0′0″W (96 grid cells)	Historical: 24.2 SSP1-2.6: 25.8 SSP5-8.5: 29.3	Historical: 195 SSP1-2.6: 200 SSP5-8.5: 191	Historical: 8.71 SSP1-2.6: 10.1 SSP5-8.5: 12.9	64.1
Namibia (BSh)	Lat.: 22°0′0″S, 17°0′0″S Lon.: 16°0′0″E, 21°0′0″E (90 grid cells)	Historical: 20.5 SSP1-2.6: 22.9 SSP5-8.5: 27.2	Historical: 35.6 SSP1-2.6: 31.0 SSP5-8.5: 24.3	Historical: 1.32 SSP1-2.6: 1.22 SSP5-8.5: 1.15	32.3
France (Cfb)	Lat.: 46°0′0″N, 49°0′0″N Lon.: 1°0′0″W, 6°0′0″E (84 grid cells)	Historical: 10.4 SSP1-2.6: 12.1 SSP5-8.5: 14.8	Historical: 76.3 SSP1-2.6: 76.7 SSP5-8.5: 78.3	Historical: 2.6 SSP1-2.6: 3.11 SSP5-8.5: 4.61	376
Finland (Dfc)	Lat.: 61°0′0″N, 69°0′0″N Lon.: 25°30′0″E, 28°30′0″E (96 grid cells)	Historical: 0.02 SSP1-2.6: 2.92 SSP5-8.5: 6.34	Historical: 50.2 SSP1-2.6: 56.2 SSP5-8.5: 62.3	Historical: 2.68 SSP1-2.6: 3.39 SSP5-8.5: 5.25	109

The 'Madingley' model is a process-based GEM that simulates ecosystems containing all autotroph and heterotroph organisms (with body mass ranging from 10 µg to 150 000 kg) on a global scale (Harfoot et al. 2014). We used 'MadingleyR' ver. 1.0.5 (Hoeks et al. 2021), an R implementation of the terrestrial realm of the 'Madingley' model, to conduct the simulation experiments. The 'MadingleyR' environment consists of a land surface raster layer, combined with raster layers providing environmental climate information (Harfoot et al. 2014). This includes input data for available water capacity, NPP, HANPP, near-surface temperature, diurnal temperature range, precipitation and ground frost frequency.

'MadingleyR' aggregates autotrophs and heterotrophs into cohorts and stocks within a grid cell to allow spatially explicit simulations. A stock represents the total biomass of autotrophic organisms, whereas a cohort represents a group of heterotrophic individuals with identical traits that occur in the same grid cell. Each stock or cohort represents organisms with similar functional traits grouped into specific functional groups, which are defined based on the following categorical or continuous traits (Harfoot et al. 2014):

- feeding mode (carnivore, herbivore, omnivore),
- reproductive type (semelparous, iteroparous),
- thermoregulation (ectotherm, endotherm),
- mobility (planktonic, mobile),
- assimilation efficiency, or
- body mass characteristics.

Thus, nine functional groups, namely ectothermic iteroparous carnivores, herbivores or omnivores; ectothermic semelparous carnivores, herbivores or omnivores; and endothermic carnivores, herbivores and omnivores, were considered.

In 'MadingleyR', autotroph biomass of stocks is modelled per grid cell, using a terrestrial carbon model (Smith et al. 2013), and NPP is modeled from annual precipitation and temperature averages data based on the Miami model (Lieth 1975). This method estimates NPP as a function of monthly NPP layers, precipitation, and near-surface temperature (Harfoot et al. 2014).

To simulate biomass extraction owing to land use, HANPP was applied as a factor to reduce the autotrophic biomass produced at each time step in the model (Eq. 1, adapted and modified from Harfoot et al. (2014)).

$$B_l\left(t+\Delta t\right) = B_l\left(t\right) + \Delta B_l^{\text{Growth}} \times \left(1-\Delta\text{HANPP}\right) - \Delta B_l^{\text{Mort}} \quad (1)$$

Here, B_l represents the leaf biomass, Δt a time step, $\Delta B_l^{\text{Growth}}$ the biomass growth rate, and ΔB_l^{Mort} the biomass mortality (Harfoot et al. 2014).

Each grid cell process, such as feeding, predator–prey interactions, mortality, and reproduction, is applied to each cohort, most of which are temperature-dependent. For instance, feeding interactions and growth in 'MadingleyR' depend on an activity parameter, i.e. the time during which a functional group can be considered active. While endotherms are assumed to be active at all times, temperature limits determine ectotherm activity (Deutsch et al. 2008, Harfoot et al. 2014). Metabolic loss is influenced by temperature and was modeled using the body mass and temperature relationship (Brown et al. 2004). When ectotherms are active, field metabolic rates determine energy expenditure during various activities such as dispersal and reproduction, and during periods of inactivity, basal metabolic rates determine the minimal energy requirements for maintenance (Harfoot et al. 2014). These processes, among others, determine whether heterotrophic organisms increase their body mass, biomass and abundance (Harfoot et al. 2014, Hoeks et al. 2021).

'MadingleyR' proved to reproduce real-world patterns of ecosystem structure (Harfoot et al. 2014), such as estimating reasonable ecosystem dynamics resulting from bushmeat removal through increased harvest of duiker species (Barychka et al. 2021), or helping to gain insight into the potential consequences of trophic rewilding (Hoeks et al. 2023). The ability of 'MadingleyR' to reproduce biodiversity patterns and simulate trophic dynamics and biomass fluxes across spatial scales makes it an ideal candidate for testing the complex interactive effects of anthropogenic pressures on ecosystems (Harfoot et al. 2014, Cabral et al. 2017).

Simulation experiments

We performed three different simulation experiments, incorporating 1) climate change, 2) climate change with current land use and 3) climate change with maximum land-use intensity (Fig. 1). This allowed us to analyze climate change, current land use, and maximum land use as separate drivers, as well as their combined effects on functional groups.

Each simulation experiment was run for 200 years to allow the model to reach a stable state (Fig. 1b), with a maximum of 1000 cohorts allowed simultaneously within each grid cell. Ten replicates were run for each simulation experiment, which were averaged before analyzing the results to account for variations in the output owing to stochastic processes within the model.

First, we determined the effects of climate change on an undisturbed ecosystem by replacing the standard spatial input of 'MadingleyR' for NPP, near-surface temperature, precipitation, and diurnal temperature range with the data of the three climate scenarios (step 1, Fig. 1a). This was considered a spin-up simulation allowing the model to reach a stable state. The output was used as a starting point for two further simulation experiments that applied current and maximum land-use intensity. To compare the impact of climate change as an isolated driver without other perturbations, we used the historical climate scenario as a reference point for assessing functional groups and their species characteristics.

Second, in step 2, we applied HANPP to assess the impact of current land use using the initial simulation output of each climate scenario and compared the results with the initial

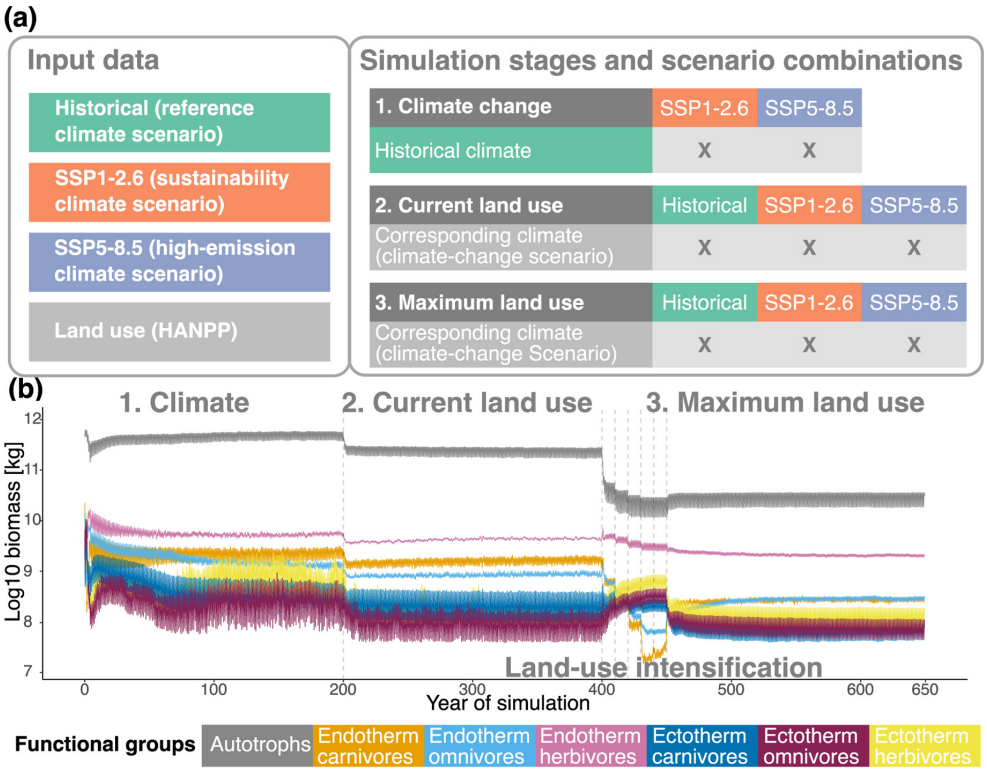

Figure 1. (a) Input data used are shown on the left, the simulation runs performed are shown on the right. Each simulation run was performed for three climate scenarios, namely, historical, SSP1-2.6, and SSP5-8.5 scenarios, to consider the combined effects of climate change and land use simultaneously (current and maximum land-use experiments) and separately (climate-change simulation). (b) The changing biomass trends under the historical climate scenario in France are shown for each functional group and autotroph organism for each consecutive simulation experiment. The three simulation experiments for climate change, current land use, and maximum land use were each run for 200 years. For intermediate land-use intensification, the model was run in 10 yearly steps for 50 years in France, resulting in a total simulation time of 650 years. This setting varies according to the minimum HANPP value across all grid cells for each region.

simulation for each climate scenario. Because HANPP quantifies the current amount of biomass removed from an ecosystem by humans, it is a measure of anthropogenic impacts on NPP (Haberl et al. 2007). Therefore, it can be interpreted as an indicator of present land-use intensity.

Third, to gradually increase land-use intensity, we built on the output of the second simulation and modified the spatial HANPP input layer of 'MadingleyR' for the simulation experiment 3.

To simulate the maximum land-use intensity, HANPP was maximized. Starting from the end point of the simulation experiment 2, HANPP was increased to a maximum of 90 in 10% steps, while running the model for 10 years per intensity step, gradually increasing the land-use intensity. The model was then run for an additional 200 years in step 3, maintaining the land-use intensity at 90% to allow the model to return to a stable state after perturbations.

Figure 1b shows a representative simulation setup, for France. The 200-year climate change experiment was followed by the 200-year current land-use experiment when land-use intensification starts. This intermediate land-use intensification simulation increased the HANPP for each grid cell within the regions according to Eq. 1, from the current HANPP. Consequently, the simulation times for land-use intensification depended on the initial HANPP values within each region. In France, for instance, only five steps were required to increase the HANPP in all grid cells to 90% intensity. The model was then run for another 200 years in step 3, maintaining the land-use intensity at 90% to allow the model to reach a new stable state. This resulted in a total simulation period of 650 years for France.

Statistical analysis

Simulations and data analyses were performed using R (ver. 4.1.2 (www.r-project.org)). 'MadingleyR' provides monthly biomass in kg for each functional group as time series. We selected the biomass outputs from the last 10 years of each simulation experiment to generate observations for our analysis. The six semelparous and iteroparous functional groups of 'MadingleyR' were grouped into ectothermic carnivores, herbivores and omnivores, resulting in three ectothermic functional groups. Biomass data were log10-transformed to account for a wide range of values. The exponentiated log response ratio (logRR) with a 0.95 studentized confidence interval was calculated by bootstrapping 10 000 times to

quantify the magnitude of differences in biomass between scenarios for each functional group (R package 'boot', ver. 1.3.28) (Davison and Hinkley 1997, Canty and Ripley 2022). LogRR is the ratio of the difference between control and experimental groups (Hedges et al. 1999). LogRR was calculated as described by Lajeunesse (2011).

$$\text{logRR} = \ln\left(\frac{X_T}{X_C}\right) \quad (2)$$

Here, X_T is the experimental group and X_C is the control group. To analyze the effects of climate change, we used the historical climate simulation as the control (Fig. 1a (1, historical)). For current land use, we used the climate simulation without land use (Fig. 1a (1)), and for maximum land use, we used the simulation with current land use under the corresponding climate scenario as the control (Fig. 1a (2)). We then calculated the percentage change in the effect size relative to the control from the logRR (Pustejovsky 2018). Changes in the power law between body mass and abundance (Blackburn and Gaston 1999, White et al. 2007, Lewis et al. 2008) were analyzed by spatial regression using the 'spatialreg' package, ver. 1.3.2 (Pebesma and Bivand 2023). To generate sample sizes for each simulation experiment, the output of the last simulation year was averaged across replicates, grid cells, and functional groups to generate an average for each functional group within a grid cell. We first applied a linear regression using abundance as the response variable and the body mass (expressed in kilograms in the previous step) of each functional group as the explanatory variable. Both variables were log10-transformed. Because abundance in the 'MadingleyR' model is influenced by cohorts dispersing between grid cells, and grid cells are influenced by spatial landscape information (Harfoot et al. 2014, Hoeks et al. 2021), we found significant autocorrelation in both the response variable and the residuals. Hence, a combined spatial autoregressive model was constructed for each region, functional group, and simulation experiment. To account for the autocorrelation, a spatial weight object was created based on the grid of each region, assuming queen adjacency between grid cells, using the 'spdep' package ver. 1.3.3 (Pebesma and Bivand 2023). Finally, the slope and p-values with a significance level of $p < 0.05$ were extracted from each model to generate a heat map plot. Further methodological details and all other statistical values of the combined spatial autoregressive models not included in the Results section can be found in the Supporting information.

Results

Impacts on total biomass

Figure 2 shows the impact of each climate scenario on the total biomass of each region, as simulated in the three experiments. Compared to the biomass in the historical climate scenario, biomass decreased in the SSP1-2.6 and SSP5-8.5 (Fig. 2a) scenarios in all regions except Finland, where the SSP1-2.6 scenario presented a change of + 0.03%. The largest decrease was observed in the arid climate zone of Namibia, with −2.13 and −0.87% in the SSP5-8.5 and SSP1-2.6 climate scenarios, respectively. The second-largest decrease across regions was observed in the tropical climate of Brazil,

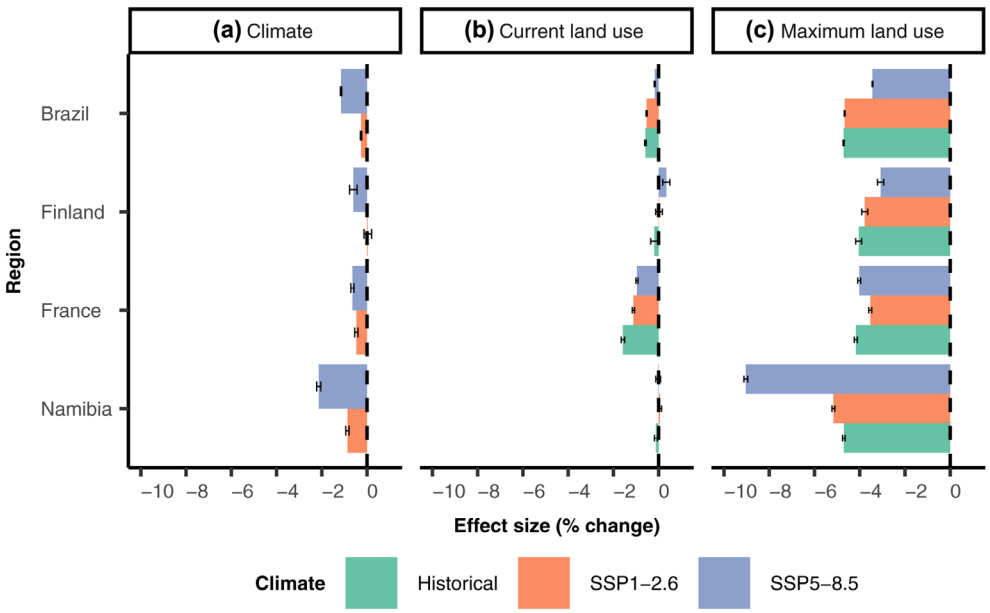

Figure 2. Percentage changes in the total biomass for each region. (a) With no land use (climate) using the historical climate scenario as the control, (b) with current land use using the climate scenario in (a) as the control, and (c) with maximum land-use intensity using the current land-use output in (b) as the control. The x-axis shows the percentage change in biomass relative to the control, and the y-axis indicates the regions. Error bars show the bootstrapped 95% confidence intervals of the effect sizes.

with −1.15% biomass in the SSP5-8.5 scenario. The negative impact of SSP1-2.6 was higher in France (−0.47%) than in Brazil (−0.26%). In general, biomass was reduced to a greater extent in the SSP5-8.5 than in the SSP1-2.6 climate scenario across all regions.

Simulations based on current land-use intensity (Fig. 2b) led to almost no change in biomass in Namibia (−0.12% for the historical scenario and +0.05% for the SSP1-2.6 scenario) and Finland (−0.19% for the historical scenario and +0.34% for the SSP5-8.5 scenario). Across all regions, the largest decrease in biomass in the historical climate scenario was observed in France (−1.58%), which had the most intense current land use (highest HANPP; Table 1), followed by Brazil (−0.58%). For all regions, the historical climate combined with current land use had the largest negative impact on total biomass. However, the negative impact of the SSP5-8.5 scenario was higher than the impact of current land use in Brazil, Namibia and Finland during the simulations.

Simulation of maximum land-use intensity led to a decrease in biomass in all regions (Fig. 2c). The biomass decrease ranged from −3.1% in Finland to −9% in Namibia, both under the SSP5-8.5 climate scenario). In Namibia, which had the lowest NPP (Table 1), the SSP5-8.5 climate scenario led to the largest decrease in biomass, while in the other regions, the decrease was higher under the historical climate scenario.

Impacts on biomass by functional groups

Across all regions, the effect of climate change on functional group biomass ranged from −7.42% (ectothermic herbivores, France, Fig. 3c(a)) to +1.75% (ectothermic herbivores, Finland, Fig. 3b(a)) and from −3.75% (ectothermic herbivores, Namibia, Fig. 3d(a)) to +0.25% (endothermic carnivores, Finland, Fig. 3b(a)) under the SSP5-8.5 and SSP1-2.6 climate scenarios, respectively.

The biomass decreased for all ectotherm groups except for the ectothermic herbivores (+1.75%; Fig. 3b(a)) and omnivores (+0.03%; Fig. 3b(a)) in Finland under the SSP5-8.5 scenario. A similar effect was observed for the endothermic functional groups, all of which decreased slightly in biomass, except for endothermic herbivores in Brazil (+0.02%; Fig. 3a(a)) and endothermic omnivores in France (+0.24%; Fig. 3c(a)).

Compared to SSP5-8.5, the biomass was less reduced in the SSP1-2.6 scenario. However, all ectothermic functional groups were slightly reduced in biomass (ranging from −0.33% for ectothermic carnivores in France to −3.75% for ectothermic herbivores in Namibia, Fig. 3c(a), d(a)), whereas the endothermic functional groups partly gained biomass (up to +0.25% for endothermic carnivores in Finland, Fig. 3b(a)).

Unlike the separate effects of the climate scenarios, the effect of current land use strongly depended on the current HANPP and was therefore the largest in France (highest HANPP; Table 1) and smallest in Namibia (lowest HANPP; Table 1). The maximum effect ranged from −7.99% for ectothermic herbivores in France (Fig. 3c(b)) to +0.89% for endothermic carnivores in Namibia, both under the historical climate scenario (Fig. 3d(b)). Ectotherms, except for ectothermic omnivores in Namibia, decreased in biomass under both future climate scenarios (+0.17% in SSP1-2.6 and +0.72% in SSP5-8.5; Fig. 3d(b)).

The largest negative impacts of land-use intensification on biomass were observed for endothermic carnivores in Finland (Fig. 3b(c)), where endothermic carnivores became extinct under all climate scenarios, and in Namibia (Fig. 3d(c)), where endothermic carnivores and omnivores became extinct under the SSP1-2.6 and SSP5-8.5 climate scenarios. Changes in the biomass of ectotherm species ranged from +2.29% for ectothermic herbivores in Finland (under the climate scenario SSP1-2.6, Fig. 3b(c)) to −18.03% for ectothermic carnivores in Namibia (under the climate scenario SSP5-8.5, Fig. 3d(c)). In contrast, endothermic species lost biomass, with the loss ranging from −1.39% for endothermic herbivores in Finland (under SSP5-8.5, Fig. 3b(c)) to −20.47% for endothermic omnivores in Namibia (under the historical climate scenario, Fig. 3d(c)). Both endothermic and ectothermic carnivores were the functional groups most negatively affected by the maximum land-use intensity, except for Brazil (Fig. 3a(c)), where it was highly dependent on the climate scenario (carnivores were most affected only under the SSP5-8.5 future climate scenario).

Impacts on the abundance–body mass relationships

Figure 4 shows the slopes of the power law between abundance and body mass. A negative slope indicates a decrease in body mass with increasing abundance. Most correlations in the climate and current land-use simulations were not significant, whereas in the maximum land-use experiment, all results were significant except those for ectothermic omnivores in Brazil and ectothermic carnivores in Namibia, both under the SSP5-8.5 climate scenario, as well as for ectothermic herbivores in France under the historical and SSP1-2.6 climate scenarios. The significant correlations between abundance and body mass are described below. In the climate change experiment, the slopes were the lowest in Namibia, indicating that high abundance decreased steeply with increasing body mass (up to −13.22 for ectothermic herbivores under the historical climate scenario). The largest slope was observed in Finland (a maximum of 1.63 for ectothermic omnivores under the SSP5-8.5 climate). On comparing the results across regions, ectothermic functional groups had lower slopes in France and Namibia (i.e. higher abundances with decreasing body mass) than endothermic functional groups (except for ectothermic carnivores in Namibia under the historical and SSP5-8.5 climate scenarios). Under the SSP1-2.6 climate scenario, slopes decreased for endothermic carnivores in Brazil. Under the SSP5-8.5 climate scenario, slopes decreased for endothermic carnivores in Finland and ectothermic omnivores in Namibia. Apart from these exceptions, the slopes increased under both the future climate scenarios SSP1-2.6 and SSP5-8.5.

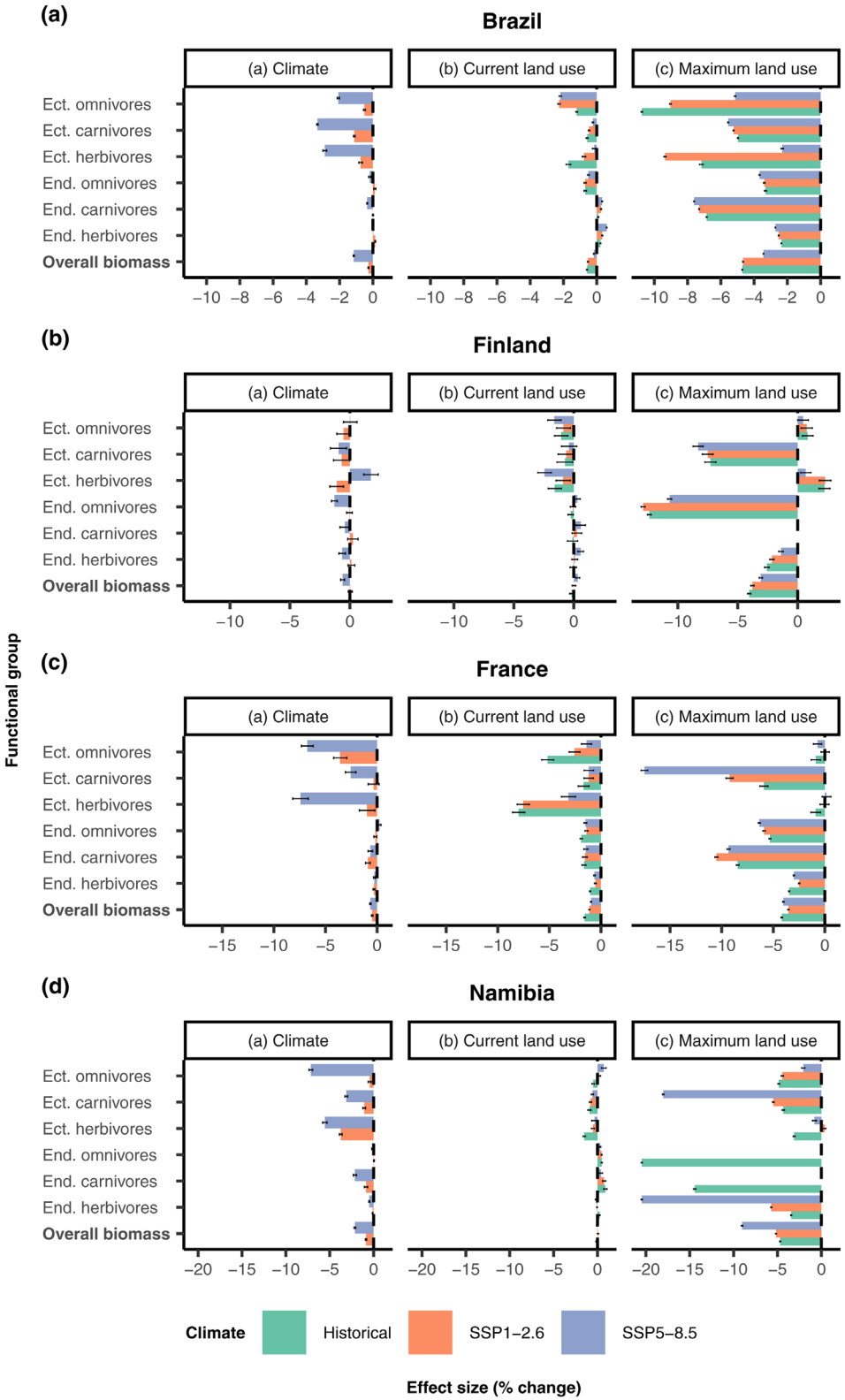

Figure 3. Percentage change in biomass for each functional group and region (a–d). (a) (Climate) with no land use using historical climate scenario as the control, (b) with current land use using the climate scenario from (a) as the control, and (c) with maximum land-use intensity using current land-use output in (b) as the control. The x-axis of each plot shows the percentage change in biomass relative to the control, and the y-axis shows the functional groups, where 'Ect.' denotes ectotherm and 'End.' denotes endotherm species. Error bars show the bootstrapped 95% confidence intervals of the effect sizes.

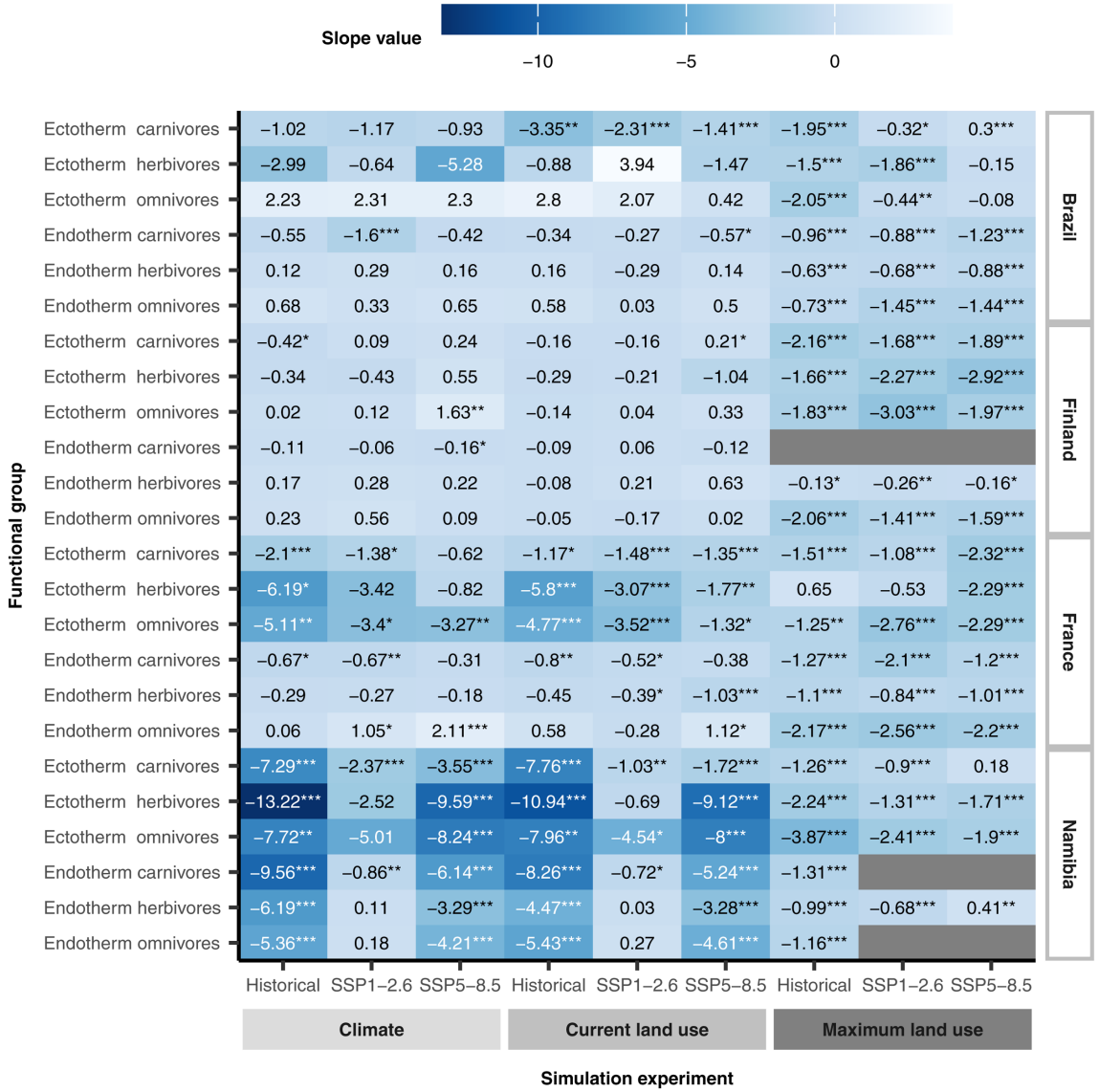

Figure 4. Heatmap of the slopes of the combined spatial autoregressive models using abundance and body mass as the dependent and explanatory variables, respectively. Results are displayed for each simulation experiment in terms of each region, functional group, and climate scenario. The x-axis shows the simulation experiments and the climate scenarios. The y-axis shows the functional group on the left side, and the region on the right side. Slope values are displayed at the top. A negative slope indicates decreasing body mass with increasing abundance, and a positive slope indicates increasing body mass with decreasing abundance. Asterisks denote significance levels: * indicates significance with p-values < 0.05, ** indicates very significant p-values < 0.01, and *** indicates highly significant p-values < 0.001.

During the current land-use simulation, most slopes decreased under the SSP5-8.5 climate scenario. The slopes decreased in Brazil, Finland and France (except for the ectothermic omnivores). In contrast, the slopes increased in Namibia (except for endothermic omnivores) under the SSP5-8.5 climate scenario. In all regions, slopes increased to the same extent under the historical and SSP5-8.5 climate scenarios and decreased the most under the SSP5-8.5 climate scenario when combined with current land use.

Finally, in the maximum land-use experiment, slopes decreased in all regions, except for Namibia, where all slopes increased, except for endothermic herbivores under the SSP1-2.6 climate scenario. In Brazil (except for endothermic omnivores under the SSP1-2.6 climate scenario), Finland and France, all endothermic functional groups decreased in slope, indicating a shift in body mass towards smaller endotherms. In Finland, the slopes of all ectothermic functional groups decreased in slope. In France, this occurred only for ectothermic carnivores and omnivores under the SSP5-8.5 climate scenario and in Brazil for ectothermic omnivores and carnivores under the historical climate scenario and for ectothermic herbivores under the SSP1-2.6 climate scenario. In Namibia, the slopes increased for all ectotherms.

Discussion

Impacts on functional groups and regions

The results supported our first hypothesis that ectotherms are the most sensitive to climate change, supporting previous findings (Kingsolver et al. 2013, Paaijmans et al. 2013, Burraco et al. 2020). The physiology of ectotherms render them vulnerable to temperature-induced changes with respect to their activity and productivity (Deutsch et al. 2008, Kingsolver et al. 2013, Paaijmans et al. 2013). In contrast, endotherms are more negatively affected by resource limitations because of their higher energy requirements for thermoregulation and larger body sizes (Nagy 2005, Buckley et al. 2012). Consequently, maximum land-use intensity was found to reduce endothermic biomass more than ectothermic biomass in Finland, and partly in France and Namibia.

Land use is also expected to affect larger organisms more than smaller ones (Bartlett et al. 2016, Ripple et al. 2016, Newbold et al. 2020a). We confirmed that increased land-use intensity leads to the downsizing of endotherms (Sheridan and Bickford 2011, Ripple et al. 2016, Enquist et al. 2020), consistent with the principles of metabolic theory (Allen et al. 2002, Brown et al. 2004).

In contrast, the positive slopes in the climate-change and current land-use simulations indicated a non-consistent power law relationship between body mass and abundance (Blackburn and Gaston 1999, White et al. 2007, Lewis et al. 2008). However, the universality of the energy equivalence rule can be undermined by specific functional groups and varying levels of anthropogenic pressures (Munn et al. 2013, Santini and Isaac 2021, Antunes et al. 2023). Notably, the simulations under the SSP1-2.6 and SSP5-8.5 climate scenarios showed that climate change may further weaken these relationships (Antunes et al. 2023), because the metabolic rates of smaller animals increase with temperature more rapidly (Johnston and Sibly 2020, Antunes et al. 2023).

In accordance with our third hypothesis, carnivores were most negatively affected by maximum land-use intensity in all regions (except for ectothermic omnivores in Brazil), culminating in the extinction of endothermic carnivores in Finland and in Namibia under the SSP1-2.6 or SSP5-8.5 climate scenarios. Thus, higher trophic levels, particularly carnivores, appear to be more vulnerable to land use (Ripple et al. 2014, Barnes et al. 2017, Newbold et al. 2020a). The results also showed that the biomass of ectothermic herbivores and omnivores may partially increase in Finland. The increase in ectotherm omnivores in Finland indicates a release of generalist mesopredators (Prugh et al. 2009, Hoeks et al. 2020). Both could be a response to the decline in top–down controlling predators (Hoeks et al. 2020) and increase the pressure on autotroph species (Botella et al. 2024). Combined with trophic downgrading, this may lead to altered top–down and bottom–up mechanisms and further relevant trophic restructuring of ecosystems (Barnes et al. 2017, Hoeks et al. 2020).

Finally, we confirmed our hypothesis that climate change has a greater impact on the total biomass of species in tropical and arid climates than on the biomass of species in other climatic zones. In both tropical (Brazil) and arid (Namibia) climates, SSP5-8.5 impacted the total biomass more negatively than the SSP1-2.6 future climate scenario. In tropical regions, the temperature range for achieving the ectotherm critical temperature is small, and the limit is rapidly reached (Deutsch et al. 2008, Buckley et al. 2012, Kingsolver et al. 2013); consequently, the rising temperatures under the SSP5-8.5 climate scenario appear to push ectotherms closer to their limits than the changes under the SSP1-2.6 scenario.

Slightly greater effects of rising temperatures were observed on the endotherms in the arid regions than on the endotherms in other regions. Of all the regions studied, the temperature increase was the highest in Namibia (Table 1), and hence, endotherms require more energy to maintain their body temperatures (Buckley et al. 2012, Kronfeld-Schor and Dayan 2013). Drought-induced low NPP (Cao et al. 2022) (SSP5-8.5, Table 1) can further decrease autotrophic biomass (Rosenblatt et al. 2017), leading to higher biomass loss in endotherms in arid regions than in other regions because of energy restrictions (Buckley et al. 2012) resulting from increasing resource limitations.

Our results also indicated that regional characteristics such as low NPP or decreasing precipitation determine the magnitude of the consequences of vegetation loss resulting from land-use intensification combined with climate change on terrestrial food webs. For example, Namibia, the region with the lowest productivity and precipitation (Table 1), experienced the greatest decrease in total biomass and disappearance of endothermic omnivores and carnivores under the SSP1-2.6 and SSP5-8.5 future climate scenarios combined with maximum land-use intensity. This impact could be a result of the interactive additive effects of both drivers within our simulation experiment. Land-use intensification decreases NPP (Haberl et al. 2007), whereas low precipitation and droughts decrease it further (Cao et al. 2022). This, in turn, increases bottom–up regulatory resource limitations due to low productivity (Oksanen et al. 1981, Hopcraft et al. 2010, Welti et al. 2020), which disproportionately affects higher trophic levels (Barnes et al. 2017, Newbold et al. 2020a) and could further reduce autotroph biomass due to the loss of top–down control (Hoeks et al. 2020).

Future prospects

The results highlight the importance of GEMs as an effective tool for understanding the multiple interacting effects of anthropogenic global change on terrestrial food webs (Harfoot et al. 2014). However, our study had certain limitations. This model did not account for direct environmental impacts beyond vegetation reduction, such as landscape fragmentation or pollution (Harfoot et al. 2014, Hoeks et al. 2021). Moreover, it did not consider extreme events or natural disasters. Increased occurrences of heat waves can negatively affect animals and lead to increased pressure on food web stability (Burraco et al. 2020, Danner et al. 2021, Sharpe et al. 2022). Finally, the analysis did not cover

plant–animal interactions accompanied by habitat shifts due to climate change. This may be particularly important in the context of land-use intensification (Seppelt et al. 2020, Burian et al. 2024), as land use may suppress the ability of species to adapt to climate change (Oliver and Morecroft 2014, Gonçalves et al. 2021).

Nevertheless, the process-based assessment of GEMs goes far beyond the capability of statistical approaches (Leclère et al. 2020, Semenchuk et al. 2022, Kok et al. 2023, Pereira et al. 2024), which provide much less information regarding the responses and interactions within trophic networks to global change (Cabral et al. 2017, Johnston et al. 2019). A combination of these approaches would be beneficial for further insights.

GEMs improve our understanding of complex food web interactions affected by global change by reproducing patterns of organismal interactions across trophic levels (Pilowsky et al. 2022) and providing a process-based understanding of potential mechanisms triggered by anthropogenic perturbations (Cabral et al. 2017, Johnston 2024). Further refinement and modification, such as the coupling of 'MadingleyR' to a dynamic global vegetation model (Krause et al. 2022), may improve the ability of GEMs to assess the consequences of anthropogenic impacts on biodiversity. The above limitations must be addressed in future studies, and the 'MadingleyR' model could be improved to gain a better understanding of the consequences of global change on food webs.

Conclusions

Our simulations confirm that global change can have fundamental consequences on ecosystem biodiversity, and global-scale ecosystem simulations can help to understand these changes, considering the spatial variability of land use and climate change. Rising temperatures, changing precipitation patterns, current land use and land-use intensification can cause various changes in the structure of food webs within terrestrial ecosystems. Increases in temperature and land use more negatively impact ectotherms and organisms of higher trophic levels such as carnivores, respectively, than other organisms. Both drivers, alone or in combination, can alter top–down and bottom–up regulatory mechanisms in trophic networks. Endotherms are affected more by energy limitations during land use than by climate impacts, whereas ectotherms are threatened by rising temperatures and land use. Land-use intensification led to declining body masses of endothermic organisms in all the study regions, except Namibia. Thus, the simulation indicated a shift towards smaller body sizes within the food web with increasing land use. Furthermore, climate change appears to have slightly greater effects in tropical and arid climates, whereas land-use intensification tends to affect less-productive environments. As global change accelerates, its potential impacts on ecosystem biodiversity must be recognized. Further developments of GEMs such as 'MadingleyR' will provide increasing insight into trophic structures influenced by external perturbations. Because GEMs provide a deeper insight than classical statistical methods, their development can lead to new insights that would otherwise be lost in coarse-scale standard methods, thus contributing to biodiversity research.

Acknowledgements – We acknowledge the World Climate Research Programme, which, through its Working Group on Coupled Modelling, coordinated and promoted CMIP6. We thank the climate modeling groups for producing and making available their model output, the Earth System Grid Federation (ESGF) for archiving the data and providing access, and the multiple funding agencies that support CMIP6 and ESGF. We want to thank Selwyn Hoeks from Radbound University Nijmegen, who was very dedicated to helping with all issues upcoming with MadingleyR and made it possible to modify MadingleyR for the appropriate purposes. Open Access funding enabled and organized by Projekt DEAL.
Funding – CN received support from HORIZON EUROPE project TRANSPATH, grant/award no. 101081984.

Author contributions

Christian Neumann: Conceptualization (equal); Data curation (lead); Formal analysis (lead); Investigation (lead); Methodology (equal); Software (lead); Visualization (lead); Writing – original draft (lead); Writing – review and editing (equal). **Tuanjit Sritongchuay**: Conceptualization (supporting); Investigation (supporting); Supervision (supporting); Writing – review and editing (supporting). **Ralf Seppelt**: Conceptualization (equal); Funding acquisition (lead); Methodology (equal); Supervision (lead); Writing – original draft (supporting); Writing – review and editing (lead).

Transparent peer review

The peer review history for this article is available at https://www.webofscience.com/api/gateway/wos/peer-review/10.1111/ecog.07533.

Data availability statement

Data are available from Github: https://github.com/CNeuhub/Madingley_CC_LU (Neumann et al. 2024).

Supporting information

The Supporting information associated with this article is available with the online version.

References

Allen, A. P., Brown, J. H. and Gillooly, J. F. 2002. Global biodiversity, biochemical kinetics, and the energetic-equivalence rule. – Science 297: 1545–1548.

Antunes, A. C., Gauzens, B., Brose, U., Potapov, A. M., Jochum, M., Santini, L., Eisenhauer, N., Ferlian, O., Cesarz, S., Scheu, S. and Hirt, M. R. 2023. Environmental drivers of local abun-

dance–mass scaling in soil animal communities. – Oikos 2023: e09735.
Barnes, A. D. et al. 2017. Direct and cascading impacts of tropical land-use change on multi-trophic biodiversity. – Nat. Ecol. Evol. 1: 1511–1519.
Bartlett, L. J., Newbold, T., Purves, D. W., Tittensor, D. P. and Harfoot, M. B. J. 2016. Synergistic impacts of habitat loss and fragmentation on model ecosystems. – Proc. R. Soc. B 283: 20161027.
Barychka, T., Mace, G. M. and Purves, D. W. 2021. The Madingley general ecosystem model predicts bushmeat yields, species extinction rates and ecosystem-level impacts of bushmeat harvesting. – Oikos 130: 1930–1942.
Beck, H. E., Zimmermann, N. E., McVicar, T. R., Vergopolan, N., Berg, A. and Wood, E. F. 2018. Present and future Köppen-Geiger climate classification maps at 1-km resolution. – Sci. Data 5: 180214.
Beckmann, M., Gerstner, K., Akin-Fajiye, M., Ceauşu, S., Kambach, S., Kinlock, N. L., Phillips, H. R. P., Verhagen, W., Gurevitch, J., Klotz, S., Newbold, T., Verburg, P. H., Winter, M. and Seppelt, R. 2019. Conventional land-use intensification reduces species richness and increases production: a global meta-analysis. – Global Change Biol. 25: 1941–1956.
Blackburn, T. M. and Gaston, K. J. 1999. The relationship between animal abundance and body size: a review of the mechanisms. – Adv. Ecol. Resr 28: 181–210.
Bloor, J. M. G., Si-Moussi, S., Taberlet, P., Carrère, P. and Hedde, M. 2021. Analysis of complex trophic networks reveals the signature of land-use intensification on soil communities in agroecosystems. – Sci. Rep. 11: 18260.
Botella, C., Gaüzère, P., O'Connor, L., Ohlmann, M., Renaud, J., Dou, Y., Graham, C. H., Verburg, P. H., Maiorano, L. and Thuiller, W. 2024. Land-use intensity influences European tetrapod food webs. – Global Change Biol. 30: e17167.
Brown, J. H., Gillooly, J. F., Allen, A. P., Savage, V. M. and West, G. B. 2004. Toward a metabolic theory of ecology. – Ecology 85: 1771–1789.
Buckley, L. B., Hurlbert, A. H. and Jetz, W. 2012. Broad-scale ecological implications of ectothermy and endothermy in changing environments: ectothermy and endothermy. – Global Ecol. Biogeogr. 21: 873–885.
Burian, A., Kremen, C., Wu, J. S.-T., Beckmann, M., Bulling, M., Garibaldi, L. A., Krisztin, T., Mehrabi, Z., Ramankutty, N. and Seppelt, R. 2024. Biodiversity–production feedback effects lead to intensification traps in agricultural landscapes. – Nat. Ecol. Evol. 8: 752–760.
Burraco, P., Orizaola, G., Monaghan, P. and Metcalfe, N. B. 2020. Climate change and ageing in ectotherms. – Global Change Biol. 26: 5371–5381.
Cabral, J. S., Valente, L. and Hartig, F. 2017. Mechanistic simulation models in macroecology and biogeography: state-of-art and prospects. – Ecography 40: 267–280.
Canty, A. and Ripley, B. 2022. boot: bootstrap R (S-plus) functions. – https://CRAN.R-project.org/package=boot.
Cao, D., Zhang, J., Han, J., Zhang, T., Yang, S., Wang, J., Prodhan, F. A. and Yao, F. 2022. Projected increases in global terrestrial net primary productivity loss caused by drought under climate change. – Earths Future 10: e2022EF002681.
Chrysafi, A. et al. 2022. Quantifying Earth system interactions for sustainable food production via expert elicitation. – Nat. Sustain. 5: 830–842.
Danner, R. M., Coomes, C. M. and Derryberry, E. P. 2021. Simulated heat waves reduce cognitive and motor performance of an endotherm. – Ecol. Evol. 11: 2261–2272.
Davison, A. C. and Hinkley, D. V. 1997. Bootstrap methods and their application. – Cambridge Univ. Press.
Deutsch, C. A., Tewksbury, J. J., Huey, R. B., Sheldon, K. S., Ghalambor, C. K., Haak, D. C. and Martin, P. R. 2008. Impacts of climate warming on terrestrial ectotherms across latitude. – Proc. Natl Acad. Sci. USA 105: 6668–6672.
Enquist, B. J., Abraham, A. J., Harfoot, M. B. J., Malhi, Y. and Doughty, C. E. 2020. The megabiota are disproportionately important for biosphere functioning. – Nat. Commun. 11: 699.
Eyring, V., Bony, S., Meehl, G. A., Senior, C. A., Stevens, B., Stouffer, R. J. and Taylor, K. E. 2016. Overview of the Coupled Model Intercomparison Project Phase 6 (CMIP6) experimental design and organization. – Geosci. Model Dev. 9: 1937–1958.
Fricke, E. C., Hsieh, C., Middleton, O., Gorczynski, D., Cappello, C. D., Sanisidro, O., Rowan, J., Svenning, J.-C. and Beaudrot, L. 2022. Collapse of terrestrial mammal food webs since the Late Pleistocene. – Science 377: 1008–1011.
Gerstner, K., Dormann, C. F., Stein, A., Manceur, A. M. and Seppelt, R. 2014. Editor's choice: review: effects of land use on plant diversity – a global meta-analysis. – J. Appl. Ecol. 51: 1690–1700.
Gonçalves, F., Sales, L. P., Galetti, M. and Pires, M. M. 2021. Combined impacts of climate and land use change and the future restructuring of Neotropical bat biodiversity. – Perspect. Ecol. Conserv. 19: 454–463.
Haberl, H., Erb, K. H., Krausmann, F., Gaube, V., Bondeau, A., Plutzar, C., Gingrich, S., Lucht, W. and Fischer-Kowalski, M. 2007. Quantifying and mapping the human appropriation of net primary production in earth's terrestrial ecosystems. – Proc. Natl Acad. Sci. USA 104: 12942–12947.
Harfoot, M. B. J., Newbold, T., Tittensor, D. P., Emmott, S., Hutton, J., Lyutsarev, V., Smith, M. J., Scharlemann, J. P. W. and Purves, D. W. 2014. Emergent global patterns of ecosystem structure and function from a mechanistic general ecosystem model. – PLoS Biol. 12: e1001841.
Hayden Bofill, S. I. and Blom, M. P. K. 2024. Climate change from an ectotherm perspective: evolutionary consequences and demographic change in amphibian and reptilian populations. – Biodivers. Conserv. 33: 905–927.
Hedges, L. V., Gurevitch, J. and Curtis, P. S. 1999. The meta-analysis of response ratios in experimental ecology. – Ecology 80: 1150–1156.
Hoeks, S., Huijbregts, M. A. J., Busana, M., Harfoot, M. B. J., Svenning, J. C. and Santini, L. 2020. Mechanistic insights into the role of large carnivores for ecosystem structure and functioning. – Ecography 43: 1752–1763.
Hoeks, S., Tucker, M. A., Huijbregts, M. A. J., Harfoot, M. B. J., Bithell, M. and Santini, L. 2021. MadingleyR: an R package for mechanistic ecosystem modelling. – Global Ecol. Biogeogr. 30: 1922–1933.
Hoeks, S., Huijbregts, M. A. J., Boonman, C. C. F., Faurby, S., Svenning, J., Harfoot, M. B. J. and Santini, L. 2023. Shifts in ecosystem equilibria following trophic rewilding. – Divers. Distrib. 29: 1512–1526.
Hopcraft, J. G. C., Olff, H. and Sinclair, A. R. E. 2010. Herbivores, resources and risks: alternating regulation along primary envi-

ronmental gradients in savannas. – Trends Ecol. Evol. 25: 119–128.
Huey, R. B., Kearney, M. R., Krockenberger, A., Holtum, J. A. M., Jess, M. and Williams, S. E. 2012. Predicting organismal vulnerability to climate warming: roles of behaviour, physiology and adaptation. – Philos. Trans. R. Soc. B 367: 1665–1679.
IPBES 2019. Global assessment report on biodiversity and ecosystem services of the intergovernmental science-policy platform on biodiversity and ecosystem services. – IPBES.
IPCC 2021. Climate change 2021 – the physical science basis: working group I contribution to the sixth assessment report of the intergovernmental panel on climate change. – Cambridge Univ. Press.
Jaureguiberry, P., Titeux, N., Wiemers, M., Bowler, D. E., Coscieme, L., Golden, A. S., Guerra, C. A., Jacob, U., Takahashi, Y., Settele, J., Díaz, S., Molnár, Z. and Purvis, A. 2022. The direct drivers of recent global anthropogenic biodiversity loss. – Sci. Adv. 8: eabm9982.
Johnston, A. S. A. 2024. Predicting emergent animal biodiversity patterns across multiple scales. – Global Change Biol. 30: e17397.
Johnston, A. S. A. and Sibly, R. M. 2020. Multiple environmental controls explain global patterns in soil animal communities. – Oecologia 192: 1047–1056.
Johnston, A. S. A., Boyd, R. J., Watson, J. W., Paul, A., Evans, L. C., Gardner, E. L. and Boult, V. L. 2019. Predicting population responses to environmental change from individual-level mechanisms: towards a standardized mechanistic approach. – Proc. R. Soc. B 286: 20191916.
Kingsolver, J. G., Diamond, S. E. and Buckley, L. B. 2013. Heat stress and the fitness consequences of climate change for terrestrial ectotherms. – Funct. Ecol. 27: 1415–1423.
Kok, M. T. J., Meijer, J. R., Van Zeist, W.-J., Hilbers, J. P., Immovilli, M., Janse, J. H., Stehfest, E., Bakkenes, M., Tabeau, A., Schipper, A. M. and Alkemade, R. 2023. Assessing ambitious nature conservation strategies in a below 2-degree and food-secure world. – Biol. Conserv. 284: 110068.
Krause, J., Harfoot, M., Hoeks, S., Anthoni, P., Brown, C., Rounsevell, M. and Arneth, A. 2022. How more sophisticated leaf biomass simulations can increase the realism of modelled animal populations. – Ecol. Modell. 471: 110061.
Kronfeld-Schor, N. and Dayan, T. 2013. Thermal ecology, environments, communities, and global change: energy intake and expenditure in endotherms. – Annu. Rev. Ecol. Evol. Syst. 44: 461–480.
Lajeunessei, M. J. 2011. On the meta-analysis of response ratios for studies with correlated and multi-group designs. – Ecology 92: 2049–2055.
Lasmar, C. J., Rosa, C., Queiroz, A. C. M., Nunes, C. A., Imata, M. M. G., Alves, G. P., Nascimento, G. B., Ázara, L. N., Vieira, L., Louzada, J., Feitosa, R. M., Brescovit, A. D., Passamani, M. and Ribas, C. R. 2021. Temperature and productivity distinctly affect the species richness of ectothermic and endothermic multitrophic guilds along a tropical elevational gradient. – Oecologia 197: 243–257.
Leclère, D. et al. 2020. Bending the curve of terrestrial biodiversity needs an integrated strategy. – Nature 585: 551–556.
Lewis, H. M., Law, R. and McKane, A. J. 2008. Abundance–body size relationships: the roles of metabolism and population dynamics. – J. Anim. Ecol. 77: 1056–1062.
Lieth, H. 1975. Modeling the primary productivity of the world. – In: Lieth, H. and Whittaker, R. H. (eds), Primary productivity of the biosphere, ecological studies. Springer, pp. 237–263.
Loh, J., Green, R. E., Ricketts, T., Lamoreux, J., Jenkins, M., Kapos, V. and Randers, J. 2005. The living planet index: using species population time series to track trends in biodiversity. – Philos. Trans. R. Soc. B 360: 289–295.
Mantyka-pringle, C. S., Martin, T. G. and Rhodes, J. R. 2012. Interactions between climate and habitat loss effects on biodiversity: a systematic review and meta-analysis. – Global Change Biol. 18: 1239–1252.
Munn, A. J., Dunne, C., Müller, D. W. H. and Clauss, M. 2013. Energy in-equivalence in Australian marsupials: evidence for disruption of the continent's mammal assemblage, or are rules meant to be broken? – PLoS One 8: e57449.
Nagy, K. A. 2005. Field metabolic rate and body size. – J. Exp. Biol. 208: 1621–1625.
Neumann, C., Sritongchuay, T. and Seppelt, R. 2024. Data from: Model-based impact analysis of climate change and land-use intensification on trophic networks. – Github, https://github.com/CNeu-hub/Madingley_CC_LU.
Newbold, T. et al. 2015. Global effects of land use on local terrestrial biodiversity. – Nature 520: 45–50.
Newbold, T., Bentley, L. F., Hill, S. L. L., Edgar, M. J., Horton, M., Su, G., Şekercioğlu, Ç. H., Collen, B. and Purvis, A. 2020a. Global effects of land use on biodiversity differ among functional groups. – Funct. Ecol. 34: 684–693.
Newbold, T., Tittensor, D. P., Harfoot, M. B. J., Scharlemann, J. P. W. and Purves, D. W. 2020b. Non-linear changes in modelled terrestrial ecosystems subjected to perturbations. – Sci. Rep. 10: 14051.
O'Connor, L. M. J., Cosentino, F., Harfoot, M. B. J., Maiorano, L., Mancino, C., Pollock, L. J. and Thuiller, W. 2024. Vulnerability of terrestrial vertebrate food webs to anthropogenic threats in Europe. – Global Change Biol. 30: e17253.
O'Neill, B. C., Tebaldi, C., Van Vuuren, D. P., Eyring, V., Friedlingstein, P., Hurtt, G., Knutti, R., Kriegler, E., Lamarque, J.-F., Lowe, J., Meehl, G. A., Moss, R., Riahi, K. and Sanderson, B. M. 2016. The scenario model intercomparison project (ScenarioMIP) for CMIP6. – Geosci. Model Dev. 9: 3461–3482.
Oksanen, L., Fretwell, S. D., Arruda, J. and Niemela, P. 1981. Exploitation ecosystems in gradients of primary productivity. – Am. Nat. 118: 240–261.
Oliver, T. H. and Morecroft, M. D. 2014. Interactions between climate change and land use change on biodiversity: attribution problems, risks, and opportunities. – WIREs Clim. Change 5: 317–335.
Paaijmans, K. P., Heinig, R. L., Seliga, R. A., Blanford, J. I., Blanford, S., Murdock, C. C. and Thomas, M. B. 2013. Temperature variation makes ectotherms more sensitive to climate change. – Global Change Biol. 19: 2373–2380.
Pebesma, E. and Bivand, R. 2023. Spatial data science: with applications in R. – Chapman and Hall/CRC.
Pereira, H. M. et al. 2024. Global trends and scenarios for terrestrial biodiversity and ecosystem services from 1900 to 2050. – Science 384: 458–465.
Pilowsky, J. A., Colwell, R. K., Rahbek, C. and Fordham, D. A. 2022. Process-explicit models reveal the structure and dynamics of biodiversity patterns. – Sci. Adv. 8: eabj2271.
Prugh, L. R., Stoner, C. J., Epps, C. W., Bean, W. T., Ripple, W. J., Laliberte, A. S. and Brashares, J. S. 2009. The rise of the mesopredator. – BioScience 59: 779–791.
Pustejovsky, J. E. 2018. Using response ratios for meta-analyzing single-case designs with behavioral outcomes. – J. Sch. Psychol. 68: 99–112.
Ripple, W. J. et al. 2016. Saving the World's terrestrial megafauna. – BioScience 66: 807–812.
Ripple, W. J., Estes, J. A., Beschta, R. L., Wilmers, C. C., Ritchie, E. G., Hebblewhite, M., Berger, J., Elmhagen, B., Letnic, M.,

Nelson, M. P., Schmitz, O. J., Smith, D. W., Wallach, A. D. and Wirsing, A. J. 2014. Status and ecological effects of the World's largest carnivores. – Science 343: 1241484.

Rosenblatt, A. E., Smith-Ramesh, L. M. and Schmitz, O. J. 2017. Interactive effects of multiple climate change variables on food web dynamics: modeling the effects of changing temperature, CO_2, and water availability on a tri-trophic food web. – Food Webs 13: 98–108.

Santini, L. and Isaac, N. J. B. 2021. Rapid Anthropocene realignment of allometric scaling rules. – Ecol. Lett. 24: 1318–1327.

Schipper, A. M., Hilbers, J. P., Meijer, J. R., Antão, L. H., Benítez-López, A., Jonge, M. M. J., Leemans, L. H., Scheper, E., Alkemade, R., Doelman, J. C., Mylius, S., Stehfest, E., Vuuren, D. P., Zeist, W. J. and Huijbregts, M. A. J. 2020. Projecting terrestrial biodiversity intactness with GLOBIO 4. – Global Change Biol. 26: 760–771.

Segan, D. B., Murray, K. A. and Watson, J. E. M. 2016. A global assessment of current and future biodiversity vulnerability to habitat loss–climate change interactions. – Global Ecol. Conserv. 5: 12–21.

Semenchuk, P., Plutzar, C., Kastner, T., Matej, S., Bidoglio, G., Erb, K.-H., Essl, F., Haberl, H., Wessely, J., Krausmann, F. and Dullinger, S. 2022. Relative effects of land conversion and land-use intensity on terrestrial vertebrate diversity. – Nat. Commun. 13: 615.

Seppelt, R., Arndt, C., Beckmann, M., Martin, E. A. and Hertel, T. W. 2020. Deciphering the biodiversity–production mutualism in the global food security debate. – Trends Ecol. Evol. 35: 1011–1020.

Sharpe, L. L., Prober, S. M. and Gardner, J. L. 2022. In the hot seat: behavioral change and old-growth trees underpin an Australian songbird's response to extreme heat. – Front. Ecol. Evol. 10: 813567.

Sheridan, J. A. and Bickford, D. 2011. Shrinking body size as an ecological response to climate change. – Nat. Clim. Change 1: 401–406.

Smith, M. J., Purves, D. W., Vanderwel, M. C., Lyutsarev, V. and Emmott, S. 2013. The climate dependence of the terrestrial carbon cycle, including parameter and structural uncertainties. – Biogeosciences 10: 583–606.

Strona, G. and Bradshaw, C. J. A. 2022. Coextinctions dominate future vertebrate losses from climate and land use change. – Sci. Adv. 8: eabn4345.

Trzcinski, M. K., Srivastava, D. S., Corbara, B., Dézerald, O., Leroy, C., Carrias, J. F., Dejean, A. and Céréghino, R. 2016. The effects of food web structure on ecosystem function exceeds those of precipitation. – J. Anim. Ecol. 85: 1147–1160.

Voldoire, A. 2019a. CNRM-CERFACS CNRM-CM6-1-HR model output prepared for CMIP6 CMIP historical (No. 20191021). – Earth System Grid Federation.

Voldoire, A. 2019b. CNRM-CERFACS CNRM-CM6-1-HR model output prepared for CMIP6 ScenarioMIP ssp126 (No. 20200127). – Earth System Grid Federation.

Voldoire, A. 2019c. CNRM-CERFACS CNRM-CM6-1-HR model output prepared for CMIP6 ScenarioMIP ssp585 (No. 20191202). – Earth System Grid Federation.

Welti, E. A. R., Prather, R. M., Sanders, N. J., De Beurs, K. M. and Kaspari, M. 2020. Bottom-up when it is not top–down: predators and plants control biomass of grassland arthropods. – J. Anim. Ecol. 89: 1286–1294.

White, E. P., Ernest, S. K. M., Kerkhoff, A. J. and Enquist, B. J. 2007. Relationships between body size and abundance in ecology. – Trends Ecol. Evol. 22: 323–330.

Wiens, J. J. and Zelinka, J. 2024. How many species will Earth lose to climate change? – Global Change Biol. 30: e17125.

Williams, J. J. and Newbold, T. 2021. Vertebrate responses to human land use are influenced by their proximity to climatic tolerance limits. – Divers. Distrib. 27: 1308–1323.

Williams, J. J., Freeman, R., Spooner, F. and Newbold, T. 2022. Vertebrate population trends are influenced by interactions between land use, climatic position, habitat loss and climate change. – Global Change Biol. 28: 797–815.